Available online at www.sciencedirect.com
ScienceDirect
Journal of Photochemistry and Photobiology A: Chemistry 185 (2007) 76–85
Journal of Photochemistry and Photobiology A:Chemistry
www.elsevier.com/locate/jphotochem

Direct observation of protein residue solvation dynamics

Ajay Kumar Shaw [a], Rupa Sarkar [a], Debapriya Banerjee [a], Susanne Hintschich [b], Andy Monkman [b], Samir Kumar Pal [a,*]

[a] *Unit for Nano Science and Technology, S.N. Bose National Centre for Basic Sciences, Block JD, Sector III, Salt Lake, Kolkata 700098, India*
[b] *Department of Physics, University of Durham, UK*

Received 29 April 2006; received in revised form 13 May 2006; accepted 15 May 2006
Available online 19 June 2006

Abstract

Dynamics of solvation of chromophores attached to a protein by amino acid residues in comparison to that by water molecules has remained a long-standing problem in the field of protein solvation dynamics. An attempt to unravel the existing controversy has been made by studying the solvation dynamics of dansyl labeled proteolytic enzyme α-chymotrypsin in both native and denatured state. In the native state the dansyl probe at the surface of the protein interacts largely with the hydration water while in the denatured state the solvation relaxation of the probe in the randomly oriented polypeptide chain is mainly governed by the polar amino acid residues of the protein. A significant structural perturbation of the protein upon denaturation due to which the probe finds itself in a non-polar environment of the peptide residues is also evident from steady-state fluorescence, circular dichroism (CD) and dynamic light scattering (DLS) experiments. High-resolution streak camera has been employed in order to study dynamic fluorescence stokes shift of the dansyl probe due to hydration water and protein residues. The time scale of solvation by polar peptide residues is found to be an order of magnitude slower than that by bulk type water molecules. In order to show the effect of environmental restriction on the solvation dynamics, the protein in both native and denatured states have been encapsulated inside reverse micelles of varying degree of hydration (w_0). Simple theoretical models have been proposed in order to qualitatively understand the experimental findings. This study might invoke further research in the field of protein solvation.

Keywords: Protein solvation; Native/denatured states; Picosecond dynamics; Streak camera; Dynamic light scattering

1. Introduction

Water plays an important role in biomolecular recognition at specific sites of proteins and nucleic acids [1]. Especially, the specific and nonspecific dynamical interactions of a biological macromolecules with the water molecules (hydration water) in their close vicinity are essential for restoring biomolecular structure and functionality within a narrow range of temperature, pH and ionic strength [1,2]. In the recent past a significant efforts has been made in order to measure and understand the biomolecular surface hydration [3–7]. One of the early indications about the time scale of the dynamics of hydration came from dielectric measurements on protein solution [7]. The measurements show four distinct relaxation time constants (8.3, 40 ps, 10 ns and 80 ns) of myoglobin solution in contrast to that of bulk water (8.2 ps) at 298 K. However, the lack of spatial resolution in the dielectric relaxation studies has brought complications in the interpretation of the results. The exploration of the hydration dynamics using nuclear magnetic resonance (NMR) technique belongs to two classes of experiments [3], those involve the nuclear overhauser effect (NOE) and the nuclear magnetic relaxation dispersion (NMRD). The ability to study the dynamics of hydration at a particular site of a biomolecule is a major strength of the NOE method. Nevertheless, the intrinsic limitation of time resolution of the NOE has made dynamics accessible up to sub-nanosecond scale, reporting 500–300 ps [5,6]. On the other hand, from the frequency dependence of a typical NMRD experiment it has been possible to report the time scale in the range of 10–50 ps [3,4]. In contrast to the NOE techniques the lack of spatial resolution in the NMRD experiments has been considered as [4] one of the major limitations.

Spatial and temporal limitations of the earlier experiments impose constraints on the exploration of complete picture of biomolecular hydration dynamics, and simultane-

* Corresponding author. Fax: +91 33 2335 3477.
E-mail address: skpal@bose.res.in (S.K. Pal).

1010-6030/$ – see front matter © 2006 Elsevier B.V. All rights reserved.
doi:10.1016/j.jphotochem.2006.05.014

ously stimulated molecular dynamics (MD) simulation [8] and femtosecond-resolved fluorescence studies [2,9,10] to enter into the field. In an MD study on the hydration dynamics of a protein plastocyanin, it was observed that the rotational relaxation of the water molecules on average significantly slows down in the close proximity of the protein surface [8]. Femtosecond-resolved fluorescence studies on an extrinsic dye probe in a protein pocket explored the solvation dynamics of polar amino acid residues and/or rigid water molecules on slower time scales [9,10]. However, from these studies the time scales of surface waters of a biomolecule was not evident. Local structural perturbation of protein molecules due to docking of the extrinsic dye is also another issue for the discussion. In this context the tryptophan residues at the surface of protein molecules were found to be attractive probes for the surface hydration dynamics. The study on single tryptophan containing proteins has ruled out the complications due to spatial heterogeneity in the data analysis. In a hybrid quantum mechanical–classical MD method [11] the physical origin of fluorescence signal of tryptophan residues in various proteins has been clearly described. The potential danger of using arbitrary excitation wavelength of tryptophan residues in order to extract environmental dynamics has also been vividly discussed in a recent work [12].

A series of publications [13–16] followed by a review [2] explored dynamical time scales of surface hydration of various kinds of proteins including a sweet protein Monellin [14] by using tryptophan as fluorescent probe at the surfaces of the protein molecules. The constructed hydration correlation function from dynamical fluorescence stokes shift (FSS) of the tryptophan (Trp3) at the surface of Monellin showed two distinct time constants of 1.3 and 16 ps. In a simple theoretical model the observed hydration times were correlated with residence times of the water molecules at the surface (hydration layer) of the protein [17]. A more rigorous dynamical exchange model considering the diffusion of bulk water to the hydration layer is advanced in the literature [18]. The observed decay in the hydration correlation function ($C(t)$) was concluded to be *mainly* due to water molecules for the following experimental findings: (i) X-ray structure of native [19] and solution structure of single chain Monellin (SCM) [20] show significant surface exposure of the Trp3. From the X-ray structural analysis of (4MON) it is also evident that total number of residues within a radius of 4–6 Å from the Trp3 is 4 (Gly1, Lys44, Met42, Gln10) out of which the number of polar/charged residues is only 2 (Lys44 and Gln10). The NMR structure (1MNL) of the SCM shows existence of two residues (Glu2 and Gly1) within a radius of 4–6 Å from the Trp3 out of which only one residue (Glu2) is polar. In a recent MD simulation study from this group identified 58 unique water molecules interacting directly with Trp3 appeared within 4 Å from the center of the Trp3 indole ring during a simulation period of 140 ps. Thus the solvation relaxation of the Trp3 has an overwhelming influence from the surrounding water molecules compared to that from 2 to 3 polar amino acid side chains of Monellin. (ii) The solvation relaxation of a fluorescent probe inside a protein cavity [9,10], where polar residues of the protein molecule are expected to contribute mainly in the relaxation process shows much longer time constants. (iii) A typical relaxation time of a residue in the protein Monellin is evidenced from solvation of the probe Trp3 in the denatured Monellin [14] and rotational relaxation of the Trp3 in the native protein. The solvation dynamics of the Trp3 in the denatured Monellin shows a longer component of 56 ps in a 100 ps experimental window and assigned to be due to relaxation of random coiled structure of the protein around the tryptophan moiety. The study [14] does not rule out the possibility of inclusion of much longer solvation time constants beyond the experimental time window. The rotational relaxation time of the probe as evidenced from temporal fluorescence anisotropy measurement shows decay with a time constant of 32 ps (37%) and remains constant (63%) thereafter up to 300 ps. In the case of significant contribution of polar side chain motions in the relaxation process, slower time scales are expected in the decay of hydration correlation function.

However, in a recent MD study on the protein Monellin the role of water molecules in the slower (16 ps) hydration relaxation process has been argued. The MD study [21] made a point that the 16 ps component recovered from the femtosecond-resolved FSS experiment [14] was too slow to be from water molecules alone as NMRD [22] and other MD simulation [23,24] studies of aqueous proteins reveal up to seven times slower water dynamics at the surfaces of the proteins. Note that 16 ps component is 12 times slower than that of bulk water and reveals the dynamics of water molecules at a particular site (Trp3) of the protein Monellin. On the other hand the NMRD and MD studies reveal overall picture of water dynamics at the protein surfaces. In this context it should be mentioned that our MD simulation study [25] explored the equilibrium dynamics of water molecules in the close vicinity of the Trp3 of Monellin. The study [25] recovered a time constant of 14.3 ps in the dynamics of water molecules within a radius of 6 Å from the Trp3, which is in close agreement with the femtosecond-resolved FSS study [14]. In another recent work [26] the observed 16 ps component is assigned to be due to *highly quenched conformer*, as the component shows positive (decay) amplitude even at longer wavelengths. The argument is further supported by an experimental observation of similar decay in the fluorescence of tryptophan in a small 22-mer peptide, where the origin of the decay is proposed to be due to a rotamer of the tryptophan [27]. However, single tryptophan residue at the interface of the protein phospholipase A_2 (PLA2) shows [16]: (a) longer rise component (∼10 ps) in the fluorescence decays and hydration relaxation in the similar time scale (∼14 ps); (b) persistence of the temporal fluorescence anisotropy up to 300 ps experimental time window. The observations clearly rule out the involvement of either quenched state and/or rotamer in the observed hydration dynamics at the protein surfaces *in general*. Note that the lack of rise component in the detected fluorescence is not essential to rule out relaxation, as significant overlap of early and later time emission spectra may surpass that signature.

In the context of the above discussion it is extremely important to observe time scales of solvation of a probe by protein residues in contrast to those by mainly water molecules. Here, we have explored the time scales of solvation of a probe by polar protein residues. The fluorescent probe dansyl is covalently attached to a polypeptide chain of a protein α-chymotrypsin and

other polar residues are allowed to come closer to the probe by complete structural denaturation of the protein. The solvation dynamics is compared with that of the probe at the surface of the protein in the native state, where the dynamics is assumed to be mainly due to water molecules. The temporal anisotropy of the chromophore reflecting local microviscosity controlled diffusion of the probe in the native and the denatured protein is also correlated with the solvation dynamics. The change in the solvation and reorientational dynamics of the probe in the protein upon encapsulation in a nanocage of reverse micelle is also reported.

2. Materials and methods

2.1. Materials

The protein α-chymotrypsin (CHT) from bovine pancreas, bis(2-ethylhexyl)sulfosuccinate sodium salt (AOT) and urea were purchased from Sigma, dansyl chloride (DC) from Molecular Probes and isooctane from Romil. Samples were used as received without further purification. All the aqueous solutions were prepared in 0.1 M phosphate buffer.

2.2. Labeling of α-chymotrypsin

DC is known [28] to undergo intramolecular charge transfer (CT) and solvation. In steady state, in nonpolar solvents, the emission is strong and is mostly from the locally excited state, i.e., before charge separation. In polar solvents, the fluorescence decreases and is dominated by emission from the CT state. The solvent polarity and rigidity determine the wavelength and yield of emission, and that is why DC is a useful biological probe. A detailed molecular picture of solvation for this molecule has been given [29]. The covalent attachment of DC to CHT was achieved following the procedure from Molecular Probes [30]. Briefly, DC was first dissolved in a small amount of dimethyl formamide and then injected into the sodium bicarbonate solution (0.1 M) of CHT (pH 8.3). The reaction was terminated by adding a small amount of freshly prepared hydroxylamine (1.5 M, pH 8.5) after incubating it for 1 h at 4–8 °C with continuous stirring. The solution was then dialyzed exhaustively against 0.1 M phosphate buffer to separate adducts (DC–CHT) from any unreacted DC and its hydrolysis product. It should be noted that DC–CHT complexes (CHT:DC = 1:2) are quantitatively formed because of covalent synthesis. In order to impregnate DC labeled CHT in the AOT reverse micelle (RM) with various degrees of hydration (w_0 = [water]/[AOT]) [31,32], measured volumes of the protein solutions were injected to 2 ml of AOT–isooctane mixture. The solution of the DC labeled proteins in 9 M urea was kept for 24 h for complete denaturation.

2.3. Steady-state measurements

Steady-state absorption and emission were measured with Shimadzu Model UV-2450 spectrophotometer and Jobin Yvon Model Fluoromax-3 fluorimeter, respectively. Circular Dichroism (CD) was performed with a Spectropolarimeter from Jasco, model J-600 using 1 cm path-length quartz cell. All the experiments were done at room temperature (298 ± 1 K). Dynamic light scattering (DLS) measurements were done with Nano S Malvern instruments employing a 4 mW He–Ne laser (λ = 632.8 nm) and equipped with a thermostatted sample chamber. All the scattered photons were collected at 173° scattering angle at 298 K. The scattering intensity data were processed using the instrumental software to obtain the hydrodynamic diameter (d_H) and the size distribution of the scatterer in each sample. The instrument measures the time dependent fluctuation in intensity of light scattered from the particles in solution at a fixed scattering angle. Hydrodynamic diameters (d_H) of the particles were estimated from the intensity auto correlation function of the time-dependent fluctuation in intensity. d_H is defined as

$$d_H = kT/3\pi\eta D \quad (1)$$

where k is the Boltzmann constant, T the absolute temperature, η the viscosity and D is the translational diffusion coefficient. In a typical size distribution graph from the DLS measurement X-axis shows a distribution of size classes in nm, while the Y-axis shows the relative intensity of the scattered light. This is therefore known as an intensity distribution graph.

2.4. Time resolved measurements

All decays were taken by using picosecond-resolved time correlated single photon counting (TCSPC) technique. The system uses a picosecond diode laser and Becker and Hickel electronics; it has an instrument response function (IRF) ~60 ps. The picosecond excitation pulse from Picoquant diode laser was used at 388 nm. A liquid scatterer was used to measure the FWHM of the instrument response functions (IRF). Fluorescence from the sample was detected by a microchannel plate photo multiplier tube (MCP-PMT, Hammamatsu) after dispersion through a grating monochromator. For all decays the polarizer in the emission side was adjusted to be at 54.7° (magic angle) with respect to the polarization axis of the excitation beam. The observed fluorescence decays were fitted by using a nonlinear least squares fitting procedure (software SCIENTIST^{TM}) to a function comprising of the convolution of the instrument response function with a sum of exponentials. The purpose of the fitting was to obtain the decays in an analytic form suitable for further data analysis. For anisotropy measurements emission polarization was adjusted to be parallel or perpendicular to that of the excitation and anisotropy is defined as $r(t) = [I_{para} - GI_{perp}]/[I_{para} + 2GI_{perp}]$. The magnitude of G, the grating factor of the emission monochromator of the TCSPC system was found by using a coumarin dye in methanol and following longtime tail matching technique to be 1.1.

Picosecond emission spectroscopy was achieved using a streak camera setup. Samples were excited at 365 nm (3.4 eV) by a frequency doubled Ti:sapphire laser (Mira 900, Coherent) with an output pulse width of less than 2 ps and a repetition rate of 76.3 MHz. Perpendicular to the excitation path, the sample emission was passed through a monochromator (Acton Spectra Pro 2300i) and finally the 2D emission spectrum was detected

by the photocathode of a Hamamatsu streak camera (C5680). In these settings, the scattered excitation beam was observed with a half pulse width of 20 ps, which corresponds to the overall time resolution of the setup. This exceeds the laser pulse width because, for the presented experiments, the sweep speed of the streak apparatus was set as slow as possible in order to monitor sample emission as far as 2 ns. A spectral resolution of 4 nm has been determined using an argon calibration lamp. Finally, all images were corrected for curvature, shading and spectral response via computer. Spectra at fixed points in time were then read out as profiles of a specified image section. In the measured spectra some drops in the emission intensity (e.g. one around 2.2 eV) are due to artifact in the spectral correction.

2.5. Theory

In order to determine the local dynamics of the covalently bound chromophore we have determined the diffusion coefficient (D_{perp}) of the chromophoric motion by calculating the order parameter S as reported in the literature [33]. The faster rotational anisotropy time constant have been ascribed to the rapid internal motion of the chromophore, $(\phi_{int})^i$ and the longer correlation time to the rotational motion of the protein, ϕ_{prot}, where i refers to the number of faster rotational time constants. The formulae involved in the calculation of diffusion coefficient are

$$S^2 = B_{long}/\sum B_j, \quad (2)$$

where B_{long} and B_j correspond to the amplitude of the distributed correlation times assigned to the motions of protein and chromophore, respectively. The diffusion constant of the probe perpendicular to the protein surface is defined as

$$D_{perp} = (1 - S^2)/6\phi_{int} \quad (3)$$

The random coil structures adopted by denatured protein has its labeled dansyl group sampling through various conformations, including those that are exposed to bulk water, hydrophobic cores and charged sites. In the denatured state, the dynamics of the protein can be described using models developed for polymeric chains [34]. For this case, we consider the time correlation function for the chain's solvation energy fluctuations as a multiexponential function: $<\delta E(0)\delta E(t)> = \sum a_i \exp(-t/\tau_i)$, where δE is the fluctuation of solvation energy from the average equilibrium value and τ_i represents different solvation correlation time. An approximate estimate of τ_i can be obtained by assuming a Rouse chain dynamics for a homopolymer [35]. From this model the eigen values of the normal modes are given by

$$\lambda_1 = 3D_0 l^2\pi^2/N^2b^2, \quad l = 1, 3, 5, \ldots (N-1), \quad (4)$$

where N is the number of monomers in the chain, b^2 the mean square bond length and D_0 is the translational diffusion coefficient of a monomer. An estimate of D_0 can be obtained from the Stokes–Einstein relation with a stick boundary condition. The characteristic time constant (τ_l) corresponding to a given eigen value of a normal mode (λ_l) is given by $\tau_l = 1/\lambda_l$.

3. Results and discussion

3.1. Native and denatured DC–CHT in buffer

3.1.1. Steady-state studies

Fig. 1a shows the emission spectra of the dansyl chromophore covalently bound to native CHT (maximum at 2.39 eV, $\lambda_{max} = 529$ nm) in the buffer (pH 7) and denatured CHT (maximum at 2.35 eV, $\lambda_{max} = 519$ nm) in 9 M urea solution. Thus, we find a blue shift of about 10 nm upon denaturation of native CHT. This is a clear indication of the fact that dansyl molecules, which were covalently bound to the positively charged amino acid residues, lysines and arginines at the surface of CHT, were initially in a more polar hydration layer of the protein. Upon denaturation the native protein unfolds and assumes a random coil conformation. This in turn brings the dansyl molecules at the surface of CHT to a slightly non-polar environment of randomly oriented peptide residues causing a blue shift to occur. The blue shift may also be due to unfavorable interaction of excited state dipole with the opposing water dipoles in the protein electric field [11]. The sharp peak at 2.76 eV in Fig. 1a is due to Raman scattering. A significant structural (secondary) perturbation of CHT in 9 M urea solution is also evident from circular dichroism (CD) spectroscopic study (data not shown).

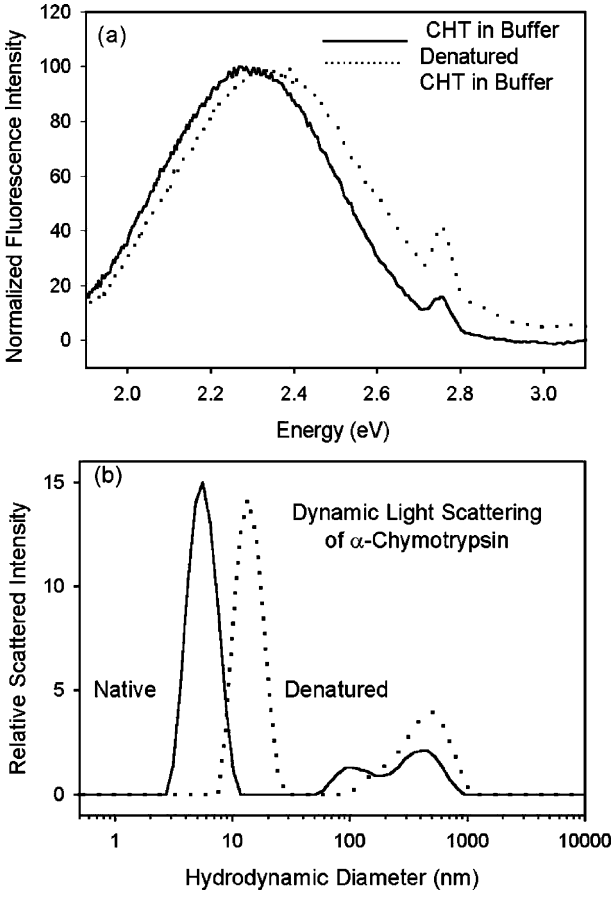

Fig. 1. (a) Steady-state emission spectra of dansyl labeled α-chymotrypsin (native and denatured). (b) Size distribution graph from dynamic light scattering for α-chymotrypsin (native and denatured).

Dynamic light scattering (DLS) studies on CHT in buffer solution shows a major scattering peak at 5.85 nm (Fig. 1b). The estimated diameter from the X-ray crystallographic (PDB code 2CHA) structure of the protein is 4.4 nm [36]. The difference in the diameters from DLS and X-ray experiments clearly reveals the thickness of the hydration layer of CHT to be ~0.73 nm. The structural perturbation in the urea solution is distinctly evidenced in Fig. 1b (dotted line). In the denaturant solution the main peak shows hydrodynamic diameter to be 12 nm indicating swelling of the protein structure upon denaturation. The peaks due to particles with higher hydrodynamic diameter (200 nm and larger) could be due to the presence of aggregates of the solutes in the solutions. Note that in the intensity distribution graph the area of the peak for the larger particles will appear at least 10^6 times larger than the peak for the smaller particles. This is because larger particles scatter much more light than smaller particles, as the intensity of scattering of a particle is proportional to the sixth power of its diameter (Rayleigh's approximation). Thus the number densities of larger particles in our solutions are negligibly small.

3.1.2. Time resolved studies

Fig. 2a shows time-resolved emission spectra (TRES) of dansyl labeled native CHT in the buffer. The center of gravity (cg) of the emission spectra just after the excitation (at time, $t = 0$) was at 2.41 eV (515 nm) and it rapidly shifts to 2.35 eV (528 nm) in 2 ns time window, which corresponds to a solvation shift of 478.1 cm^{-1}, the final wavelength being very close to the emission maxima of dansyl-CHT in the buffer (529 nm). Total estimated solvation shift of the cg as evidenced from emission spectra of DC in nonpolar and polar solvents is 3268 cm^{-1} [37], on taking the time zero emission spectrum of the probe to be similar to that in nonpolar solvent [38]. The cg of the emission spectrum of DC in a nonpolar solvent *n*-heptane is 21786.5 cm^{-1}. Thus the observed solvation shift in our time window is only 14.6% of the estimated total shift and the missing component of the dynamics in the early time due to our limited time resolution (20 ps) is 72.5%, giving an insignificant pending shift after 2 ns. Note that using femtosecond resolved fluorescence spectroscopy the longer surface hydration time constants of CHT were found to be 28 and 43 ps respectively in the active and inactive states of the protein [15]. The observation indicates that the non-specifically labeled dansyl chromophore is solvated very fast by the polar hydration layer of the protein in the native state. The dynamics may include relaxation by the collective water motion caused by protein conformational fluctuation [21]. The temporal change of the cg of the emission spectra of DC–CHT in the buffer shows single exponential decay of time constant 133.5 ps (Fig. 2c). The time constant is analogous to the solvation relaxation, which is found to be 150 ps in our previous study on CHT [37].

However, the TRES of denatured CHT (Fig. 2b) having cg of emission spectrum at 2.64 eV (470 nm at $t = 0$) shows a red shift of cg by 1356.3 cm^{-1} in 2 ns time window. The observed temporal shift (Fig. 2c), which is analogous to the solvation correlation function [37] shows a double exponential decay with a fast component 131 ps (12.9%) and a slow component of 900 ps

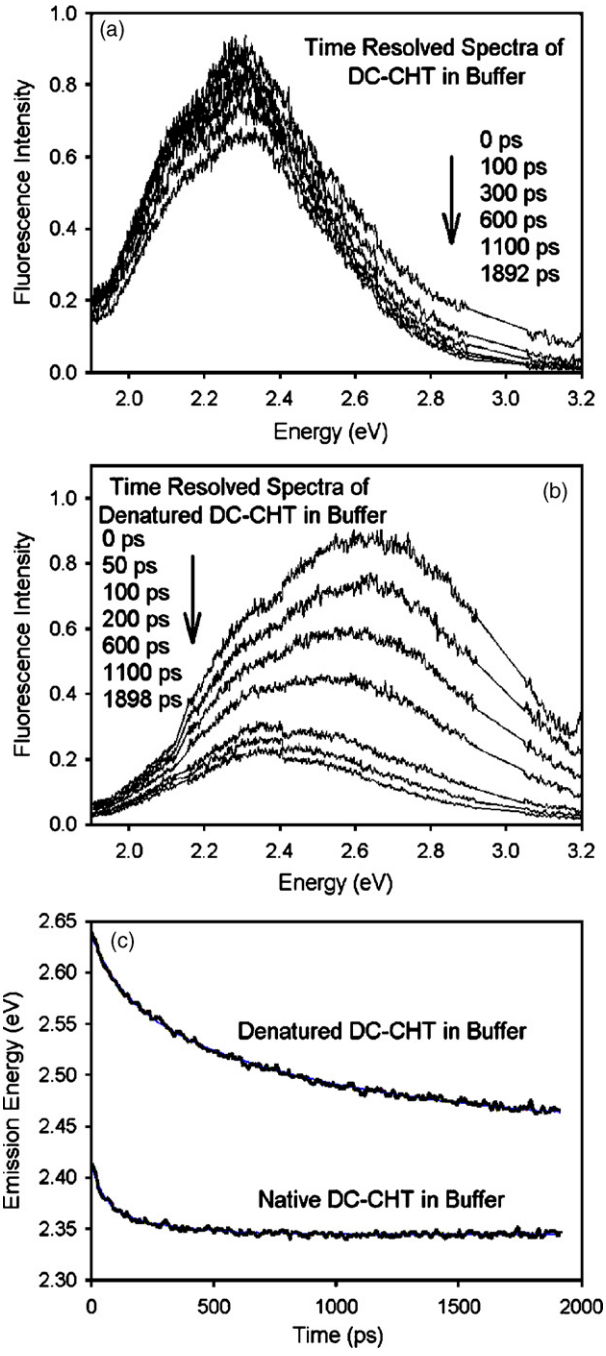

Fig. 2. (a) Time-resolved emission spectra of native dansyl labeled α-chymotrypsin in buffer. (b) Time-resolved emission spectra of denatured dansyl labeled CHT in buffer. (c) Temporal emission decay curve for native and denatured dansyl labeled CHT in the buffer.

(28.6%). The observed shift is much larger (41.5%) compared to that of the probe at the surface of the native protein (14.6%). The faster solvation time constants (~130 ps) of the native and denatured states of CHT are almost same which indicate that the faster mode of solvation is same in for both states of CHT. The slower component (900 ps) in the denatured state of the protein clearly indicates a significant contribution from the aminoacid sidechain in addition to the contribution from the water of hydration. Here the missing components in the early time due to the

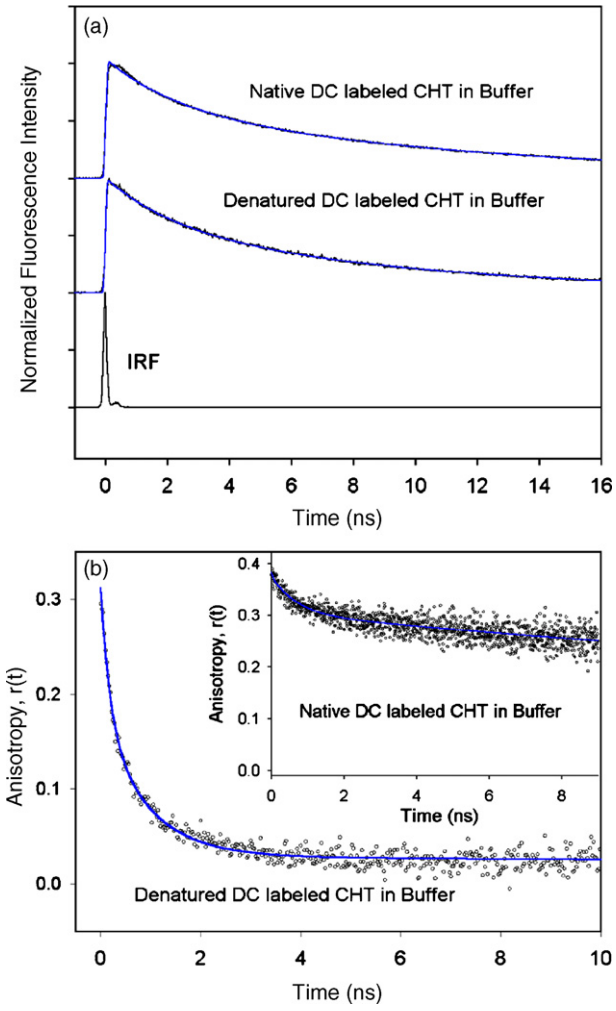

Fig. 3. (a) Fluorescence decays of dansyl labeled α-chymotrypsin (native and denatured) in buffer at 520 nm along with instrument response function (IRF). (b) Temporal anisotropy decay of native (inset) and denatured dansyl labeled α-chymotrypsin in buffer at 520 nm.

limited time resolution and after 2 ns time window are 15.6% and 42.9% of the total solvation shift respectively.

Fig. 3a shows the fluorescence decays of dansyl labeled to native CHT and urea denatured CHT measured at 520 nm. Both show a bi-exponential decay with faster components 2.2 ns (38.6%) for native CHT and 2.1 ns (36.7%) for denatured CHT while the slower component of 11.5 ns (61.4%) for native and 8.8 ns (63.3%) for denatured CHT. The faster component is due to intramolecular charge transfer while the slower component is the locally excited state lifetime of the dansyl chromophore [37]. Fig. 3b shows the temporal anisotropy decays of the dansyl in the denatured and native CHT in the (inset). From the figure it is clear that the dansyl in the native CHT is in a more restricted environment with rotational correlation time constants: 0.61 ns (21.1%) and 47.3 ns (78.9%); the initial anisotropy (r_0) at time $t = 0$ is 0.3 (see Table 1). The observation is in agreement with other studies involving specifically labeled CHT by a different probe [33]. The faster time constant corresponds to the local reorientational motion of the dansyl probe while slower one corresponds to the global motion of CHT molecule. The temporal anisotropy of the denatured CHT shows a triple exponential decay with time constants 0.18 ns (41.9%), 0.90 ns (48.4%) and 88 ns (9.7%). The faster components are considered to be the reorientational motion of the probe or segmental motion of the protein while the slower component is assigned as global motion of the denatured CHT. The closeness of the solvation times of the denatured DC–CHT with that of its two faster rotational time constants also supports the fact that upon denaturation initially buffer exposed dansyl probes find themselves in a randomly fluctuating protein environment, where they are largely relaxed by protein side chains. Diffusion coefficients of the probe calculated using Eqs. (2) and (3) are given in Table 2. From Table 2 it is evident that diffusion coefficient of the dansyl at the surface of the native CHT (0.05765 ns^{-1}) is smaller than that in the denatured protein (0.83611 and 0.16722 ns^{-1}). The observation indicates that dansyl chromophores bound to the more compact native CHT are more constrained compared to those in the denatured CHT due to random fluctuation of the protein conformation upon denaturation. Two distinct diffusion coefficients of the chromophores in the denatured state of the protein could be due to the conformational heterogeneity of the denatured protein.

Table 1
Time resolved anisotropy data for DC labeled to CHT under various conditions (numbers within parentheses denote the percentage of the component)

Sample	ϕ_1 (ns)	ϕ_2 (ns)	ϕ_3 (ns)
Native CHT in buffer	0.61 (21.1)	47.3 (78.9)	–
Denatured CHT in buffer	0.18 (41.9)	0.90 (48.4)	88.0 (9.7)
Native CHT in $w_0 = 10$ RM	0.09 (30.8)	2.03 (30.8)	50.0 (39.4)
Native CHT in $w_0 = 20$ RM	0.09 (42.2)	2.10 (22.5)	50.0 (42.3)
Denatured CHT in $w_0 = 10$ RM	0.10 (40.0)	3.13 (31.4)	45.5 (28.6)

3.2. Native and denatured α-chymotrypsin inside reverse micelles

3.2.1. Steady-state studies

In order to explore the nature of change in solvation of the probe bound to the protein in a more restricted environment,

Table 2
Calculated value of diffusion coefficient of covalently bound dansyl chromophore under various conditions

Sample	$(\phi_{int})^1$ (ns)	$(\phi_{int})^2$ (ns)	(ϕ_{prot}) (ns)	S^2	$(D_{perp})^1$ (ns^{-1})	$(D_{perp})^2$ (ns^{-1})
Native CHT in buffer	–	0.61	47.3	0.789	–	0.05765
Denatured CHT in buffer	0.18	0.90	88	0.097	0.83611	0.16722
Native CHT in $w_0 = 10$ RM	0.09	2.03	50.0	0.500	0.92593	0.04105
Native CHT in $w_0 = 20$ RM	0.09	2.10	50.0	0.500	0.92593	0.03968
Denatured CHT in $w_0 = 10$ RM	0.10	3.13	45.5	0.286	1.19000	0.03802

both the native and the denatured CHT have been encapsulated in nanometer-sized aqueous pools of AOT RM(s) of varying degree of hydration (w_0). Recent studies using circular dichroism (CD), electron paramagnetic resonance (EPR) and Fourier transformed infrared (FTIR) spectroscopy [39,40] have shown that there is an insignificant change in the structure of CHT inside RM of $w_0 = 10$ and onwards. Fig. 4a shows the emission spectra of the dansyl labeled native CHT in $w_0 = 10$ RM (maximum at 2.40 eV, $\lambda_{max} = 518$ nm) and $w_0 = 20$ RM (maximum at 2.35 eV, $\lambda_{max} = 528$ nm) and that of the denatured CHT in $w_0 = 10$ RM ($\lambda_{max} = 515$ nm). The 10 nm blue shift of emission maximum of native CHT in $w_0 = 10$ RM compared to that in $w_0 = 20$ RM indicates that in $w_0 = 10$ dansyl chromophores at the surface of CHT experience a low polarity environment due to lesser availability of bulk like water molecules. However, in $w_0 = 20$ RM, the CHT staying in the center of RM finds a more polar environment due to greater availability of bulk like water causing complete hydration [41,42]. Hence, the emission maxima of the dansyl in $w_0 = 20$ RM matches with that of the dansyl bound to the native CHT in the buffer. Upon encapsulation of the denatured CHT in $w_0 = 10$ RM, not only does the emission maximum show a greater blue shift compared to that of native CHT in $w_0 = 10$ RM but there also appears an increase in emission intensities at blue wavelengths causing the overall emission spectrum to be broad. The observation indicates that dansyl molecules in the denatured CHT in the RM find themselves in a mixed polar and non-polar environment [43,44].

3.2.2. Time resolved studies

Fig. 4b and c show the TRES of dansyl labeled native CHT in $w_0 = 10$ and 20 RM. The temporal behavior of the cg of the emission spectra of DC–CHT in the RM(s) of $w_0 = 10, 20$ are shown in Fig. 4d. Note the spectral overlap in the (2.0–2.3 eV) red side of the TRES. In a typical solvation relaxation the rate of decay in the red side is expected to be slower than that in the blue end. The absence of faster solvation decay component and presence of rise component are major reasons for the slower decay in the red end. The observed shifts are found to be 17.7% and 22.4% for $w_0 = 10$ and 20 respectively of total estimated solvation shift of 3268 cm^{-1}. The missing solvation shift in the early time (57.1% for $w_0 = 10$, and 54.7% for $w_0 = 20$) and after 2 ns time window (27.2% for $w_0 = 10$, and 22.9% for $w_0 = 20$) are comparable for both the RM(s). The temporal behavior of the emission cg of the native DC–CHT in $w_0 = 10$ shows a single exponential decay with time constant of 808 ps while that in $w_0 = 20$ shows a double exponential decay with time constants 61 ps (2.5%) and 636 ps (19.9%). From the observation it is evident that for $w_0 = 10$ RM the solvation relaxation is mainly due to bound type water molecules in the AOT/water interface in the RM. However, the DC at the surface of the protein in the RM of $w_0 = 20$ gets both the bulk type and bound interfacial type water molecules for the solvation relaxation. Fig. 5a and b show respectively the TRES and the temporal behavior of the emission cg of the dansyl labeled denatured CHT in $w_0 = 10$ RM. From the temporal behavior of the emission cg the observed shift is 15.7% of total estimated solvation shift of 3268 cm^{-1}. Significant components in the early time (49.7%) and after the 2 ns

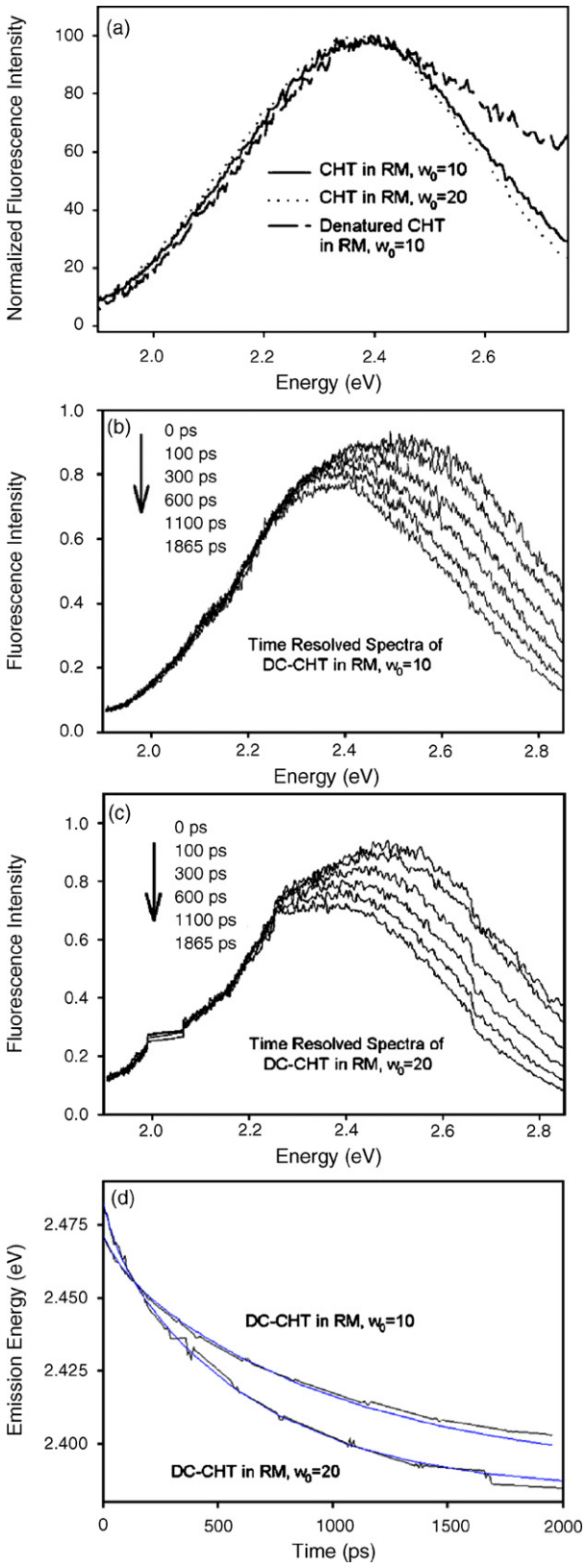

Fig. 4. (a) Steady-state emission spectra of dansyl labeled CHT in $w_0 = 10$ and 20 RM (native and denatured). (b) Time-resolved emission spectra of native dansyl labeled α-chymotrypsin in $w_0 = 10$ RM. (c) Time-resolved emission spectra of native dansyl labeled α-chymotrypsin in $w_0 = 20$ RM. (d) Temporal emission decay curve for native dansyl labeled α-chymotrypsin in $w_0 = 10$ and 20 RM.

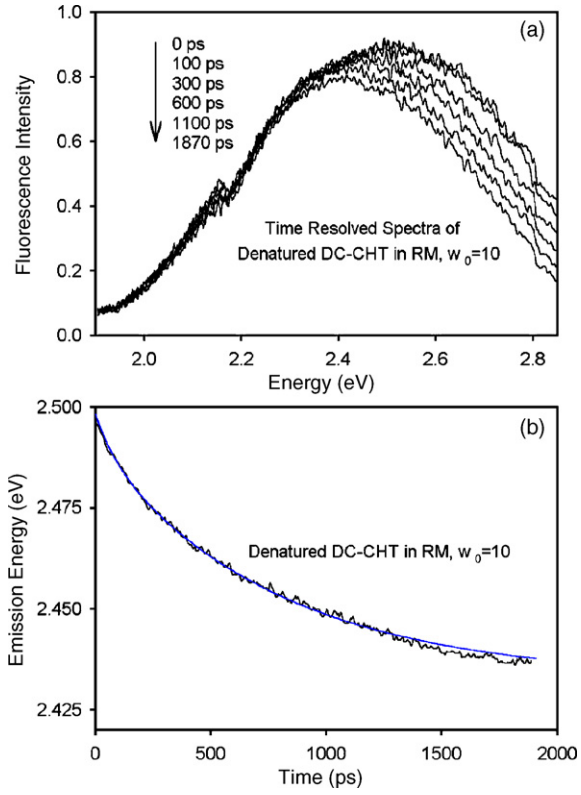

Fig. 5. (a) Time-resolved emission spectra of denatured dansyl labeled α-chymotrypsin in $w_0 = 10$ RM. (b) Temporal emission decay curve for denatured dansyl labeled α-chymotrypsin in $w_0 = 10$.

time window (34.6%) are missing. The time constants of 89 ps (2.0%) and 777 ps (13.7%) of the temporal decay of the emission cg of denatured CHT in the RM ($w_0 = 10$) differ from that of the native CHT in $w_0 = 10$ RM which somewhat ensures that denatured CHT does not get renatured upon encapsulation in the RM. The time scales of temporal anisotropy and diffusion constants of the probe dansyl in the protein upon encapsulation in the reverse micelles are tabulated in Tables 1 and 2, respectively.

In order to understand the dynamics of denatured protein and to extract the theoretical time constants due to the solvation by amino acid side residues Rouse chain model was adopted for the denatured DC–CHT in buffer and in the RM ($w_0 = 10$). The eigen values of the normal modes of the Rouse chain dynamics of the denatured protein in the buffer are estimated as follows. Here we consider $N = 245$, $b = 5$ Å and D_0 (8.3×10^{-6} cm^2 s^{-1}) [17]. The slowest and fastest time constants obtained by setting $l = 1$ and 244 in Eq. (4) are 608 and 10 ps, respectively. These time scales show that the dynamical process of the denatured CHT occurs within this time span. It is found from our calculation that the normal mode corresponding to $l = 70$ ($\tau = 124.1$ ps) and $l = 26$ ($\tau = 899.7$ ps) match very well with the faster (130.9 ps) and slower solvation time constant (899.6 ps) of the denatured CHT. Substituting the value of D_0 to be 2.3×10^{-6} cm^2 s^{-1} [41] inside the RM ($w_0 = 10$) in Eq. (2) one can obtain for $l = 1$ and 244 the dynamical time constants of protein fluctuation to be 2203 and 37 ps, respectively. Inside the RM where the viscosity is high ($\eta = 6$ cP [41]) the motion of the polar side chains of CHT is slowed down as reflected from the increased values of faster and slower time scales in comparison to that in the aqueous urea solution. The observed solvation time constants of the denatured CHT in the RM closely correspond to $l = 157$ (89.4 ps) and $l = 53$ (784.5 ps). Thus applying Rouse chain model to denatured CHT in free state and when confined in RM we can actually point out the modes of protein motion participating in solvation.

Fig. 6a shows the fluorescence decays of the dansyl labeled native CHT in $w_0 = 10$ and 20 RM and that of denatured CHT in $w_0 = 10$ RM. All the decays measured at 500 nm are biexponential in nature. The faster time constants of the native DC–CHT are 1.8 ns (27.4%) in $w_0 = 10$ RM and 1.57 ns (33.7%) in $w_0 = 20$ RM, correspond to charge transfer dynamics of dansyl chromophore while the longer time constants of 11.4 ns (72.6%) in $w_0 = 10$ and 10.62 ns (66.3%) in $w_0 = 20$ correspond to locally excited state lifetime of the chromophore. For the denatured CHT in $w_0 = 10$ RM the time constants are 2.7 ns (20.9%) and 11.9 ns (79.1%). Fig. 6b–d show the temporal anisotropy of

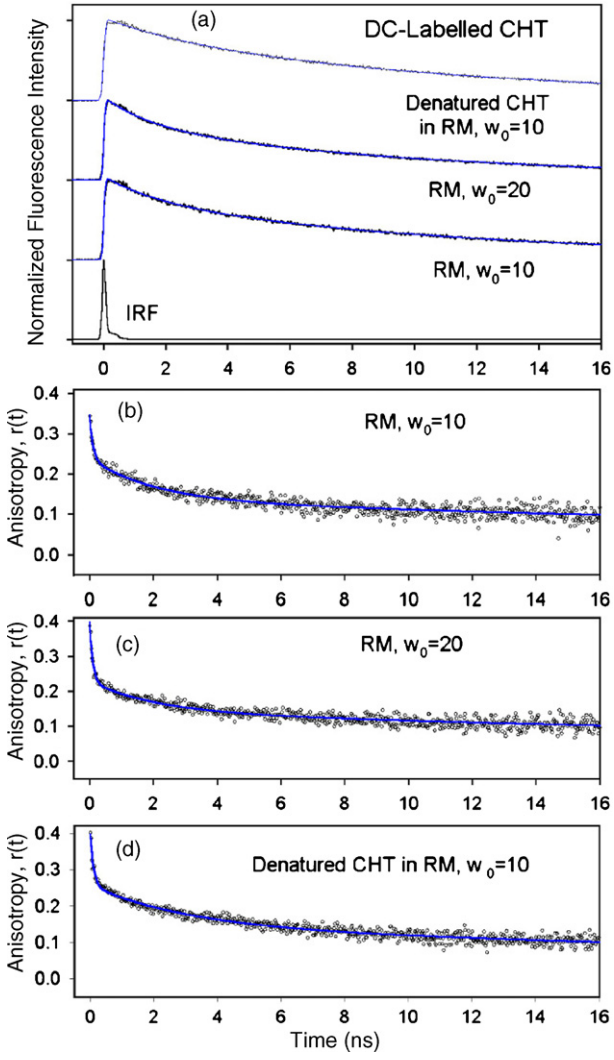

Fig. 6. (a) Fluorescent decays of dansyl labeled α-chymotrypsin (native) in $w_0 = 10$ and 20 RM and that of denatured α-chymotrypsin in $w_0 = 10$ RM at 500 nm along with instrument response function IRF. (b)–(d) show the temporal anisotropy decay of native dansyl labeled α-chymotrypsin in $w_0 = 10$, 20 RM and denatured dansyl labeled α-chymotrypsin in $w_0 = 10$, respectively at 500 nm.

native DC–CHT in $w_0 = 10, 20$ and that of denatured DC–CHT in $w_0 = 10$, respectively. From Table 1, it is found that upon incorporation of the protein in the RM the temporal anisotropy data show three rotational correlation time constants: ∼0.09, ∼2 and ∼50 ns. For native CHT in $w_0 = 10$ the 2 ns component corresponds to the local reorientational motion of the dansyl chromophore and the 50 ns component corresponds to the global motion of the protein filled RM. We find that upon incorporation of DC–CHT in the RM due to increase in local viscosity of the water pool within RM, the local orientational motion of the chromophore gets slowed down with increase in magnitude of time constant from 0.6 ns (in the buffer) to ∼2 ns (in RM). The fastest time constant of 0.09 ns may be due to the local motion of the chromophore in some perturbed site of CHT created upon incorporation in RM [39,40]. For denatured DC–CHT in $w_0 = 10$ RM, the rotational correlation time constants obtained are 0.18 ns (41.9%), 0.9 ns (48.4%) and 88 ns (9.7%). Since the compact structure of CHT is transformed into random coil, the dansyl chromophore finds itself at sites that differ widely in their local viscosities thus giving two distinct local orientational time constants. This fact is evident from the calculated diffusion coefficient of the local motion of the dansyl chromophore (see Table 2).

4. Conclusion

Studies of picosecond resolved dynamics of a covalently attached fluorescence probe at the surface of a digestive protein α-chymotrypsin and in the matrix of a randomly oriented poly peptide chain of the denatured protein elucidate the key time scales involved in the solvation of the probe by hydration water and polar residues of the protein. In the native state the probe at the surface of the protein reports a solvation time of 133.5 ps, where the dynamics is mainly due to the water molecules in the close vicinity of the protein (hydration water). Note that the solvation shift recovered in our experiment is only 14.6% with a huge missing shift of 72.5% of the total estimated dynamical fluorescence stokes shift of the probe. Earlier it has been shown that the time scale of solvation by hydration water of various protein molecules is about 20 ps [2], which is beyond our instrumental resolution. On the other hand the solvation of the probe by polar protein residues shows two distinct time constants of 130.9 and 899.6 ps, giving much slower dynamics compared to that of hydration water. Here the missing dynamics in the early time due to our limited instrumental resolution is only 15.6%. The temporal fluorescence anisotropy of the probe, which reflects a typical dynamics of a side chain in the denatured protein, is similar to dynamics of solvation of the probe in the microenvironment, reflecting significant interaction of the probe with neighboring polar residues of the protein. The rotational diffusion of the probe at the surface of the protein is found to be much retarded compared to that in the random conformation of the denatured protein.

The probe at the surface of the native protein in an aqueous nanospace of a reverse micelle ($w_0 = 10$) shows significantly slower solvation dynamics compared to that in the bulk buffer. However, upon increasing the size of the reverse micelle ($w_0 = 20$) the dynamics become faster. The faster solvation dynamics in the larger reverse micelle is consistent with the fact that the protein resides in the central water pool of the reverse micelle and in the larger sized reverse micelle the protein surface sees more bulk like water. The solvation dynamics of the probe in the denatured protein in the reverse micelle shows similar time constants to that in the bulk denaturant solution indicating a minor change of the denatured protein upon encapsulation in the nanospace. Thus, the method used in this work in order to explore key time scales of protein solvation can be effectively used in characterizing solvation patterns and dynamics of other proteins.

Acknowledgements

AKS, RS thank UGC and DB thanks CSIR for their fellowships. We acknowledge financial support from the Durham University Photonic Materials Institute and CENAMS (ONE NorthEast).

References

[1] J.A. Rupley, G. Careri, Adv. Prot. Chem. 41 (1991) 37.
[2] S.K. Pal, A.H. Zewail, Chem. Rev. 104 (2004) 2099.
[3] B. Halle, V.P. Denisov, Biopolymers 48 (1998) 210.
[4] V.P. Denisov, B. Halle, Faraday Discuss. 103 (1996) 227.
[5] K. Wüthrich, M. Billeter, P. Güntert, P. Luginbühl, R. Riek, G. Wider, Faraday Discuss. 103 (1996) 245.
[6] G. Otting, E. Liepinsh, K. Wuthrich, Science 254 (1991) 974.
[7] R.B. Gregory, Protein Solvent Interactions, Dekker, New York, 1995 (Chapter 4).
[8] C. Rocchi, A.R. Bizzarri, S. Cannistraro, Phys. Rev. E Stat. Phys. Plasmas Fluids Relat. Interdiscip. Topics 57 (1998) 3315.
[9] X.J. Jordanides, M.J. Lang, X. Song, G.R. Fleming, J. Phys. Chem. B 103 (1999) 7995.
[10] P. Changenet-Barret, C.T. Choma, E.F. Gooding, W.F. DeGrado, R.M. Hochstrasser, J. Phys. Chem. B 104 (2000) 9322.
[11] J.T. Vivian, P.R. Callis, Biophys. J. 80 (2001) 2093.
[12] X.H. Shen, J. Knutson, J. Phys. Chem. B 105 (2001) 6260.
[13] S.K. Pal, J. Peon, A.H. Zewail, Proc. Natl. Acad. Sci. U.S.A. 99 (2002) 1763.
[14] J. Peon, S.K. Pal, A.H. Zewail, PNAS, USA 99 (2002) 10964.
[15] S.K. Pal, J. Peon, A.H. Zewail, Proc. Natl. Acad. Sci. U.S.A. 99 (2002) 15297.
[16] L. Zhao, S.K. Pal, T. Xia, A.H. Zewail, Angew. Chem. Int. Ed. 43 (2004) 60.
[17] S.K. Pal, J. Peon, B. Bagchi, A.H. Zewail, J. Phys. Chem. B 106 (2002) 12376.
[18] S.M. Bhattacharyya, Z.-G. Wang, A.H. Zewail, J. Phys. Chem. B 107 (2003) 13218.
[19] G. Bujacz, M. Miller, R. Harrison, N. Thanki, G.L. Gilliland, C.M. Ogata, S.H. Kim, A. Wlodawer, Acta Crystallogr. D: Biol. Crystallogr. 53 (1997) 713.
[20] S.Y. Lee, J.H. Lee, H.J. Chang, J.M. Cho, J.W. Jung, W. Lee, Biochemistry 38 (1999) 2340.
[21] L. Nilsson, B. Halle, PNAS, USA 102 (2005) 13867.
[22] B. Halle, Philos. Trans. R. Soc. London B 359 (2004) 1207.
[23] A.R. Bizzarri, S. Cannistraro, J. Phys. Chem. B 106 (2002) 6617.
[24] M. Marchi, F. Sterpone, M. Ceccarelli, J. Am. Chem. Soc. 124 (2002) 6787.
[25] P. Hansia, S. Vishveshwara, S.K. Pal, Chem. Phys. Lett. 420 (2006) 517.
[26] J. Xu, D. Toptygin, K.J. Graver, R.A. Albertini, R.S. Savtchenko, N.D. Meadow, S. Roseman, P.R. Callis, L. Brand, J.R. Knutson, J. Am. Chem. Soc. 128 (2006) 1214.

[27] O.F.A. Larsen, I.H.M. van Stokkum, A. Pandit, R. van Grondelle, H. van Amerongen, J. Phys. Chem. B 107 (2003) 3080.
[28] B. Ren, F. Gao, Z. Tong, Y. Yan, Chem. Phys. Lett. 307 (1999) 55.
[29] D. Zhong, S.K. Pal, A.H. Zewail, ChemPhysChem 2 (2001) 219.
[30] R.P. Haugland, Handbook of Fluorescent Probes and Research Chemicals, Molecular Probes, Eugene, OR, 1996.
[31] P.L. Luisi, M. Giomini, M.P. Pileni, B.H. Robinson, Biochim. Biophys. Acta 947 (1988) 209.
[32] M.P. Pileni, Adv. Colloid Interf. Sci. 46 (1993) 139.
[33] V.N.D. Taran, C. Veeger, A.J. Visser, Eur. J. Biochem. 211 (1993) 47.
[34] M. Dio, S.F. Edwards, Theory of Polymer Dynamics, Clarendon Press, Oxford, 1986.
[35] G. Srinivas, K.L. Sebastian, B. Bagchi, J. Chem. Phys. 116 (2002) 7276.
[36] J.J. Birktoft, D.M. Blow, J. Mol. Biol. 68 (1972) 187.
[37] R. Sarkar, M. Ghosh, A.K. Shaw, S.K. Pal, J. Photochem. Photobiol. B: Biol. 79 (2005) 67.
[38] R.S. Fee, M. Maroncelli, Chem. Phys. 183 (1994) 235.
[39] A.L. Creagh, J.M. Prausnitz, H.W. Blanch, Enzyme Microb. Technol. 15 (1993) 383.
[40] J. Liu, J. Xing, R. Shen, C. Yang, H. Liu, AIChE Annual Meeting, Conference Proceeding, Austin, Texas, 2004.
[41] S.M. Andrade, S.M.B. Costa, Photochem. Photobiol. 72 (2000) 444.
[42] S.M. Andrade, S.M.B. Costa, J. Mol. Struct. 565–566 (2001) 219.
[43] D.B. Watlaufer, S.K. Malik, L. Stoller, R.L. Coffin, J. Am. Chem. Soc. 86 (1964) 508.
[44] F. Vanzi, B. Madan, K. Sharp, J. Am. Chem. Soc. 120 (1998) 10748.